JTTEE5 5:310-316


# Influence of Powder Characteristics on Plasma Sprayed Hydroxyapatite Coatings

*P. Cheang and K.A. Khor*

**Phase transformations, particle breakdown, and partial decomposition occur in hydroxyapatite (HA) powder feedstock during plasma spraying. The biological responses of the coatings consequently change from the bioactive nature of the starting material to a less biocompatible one. This paper investigates the influence of powder characteristics on the phase composition and microstructure of plasma sprayed HA coatings. The raw HA was prepared by chemically reacting calcium hydroxide with orthophosphoric acid. Subsequently, HA was either calcined and crushed, flame spheroidized, or spray dried. These three types of HA powders were plasma sprayed on steel substrates to form coatings. A previous study showed that the calcined HA powder suffered from particle breakdown in the plasma. The plasma sprayed HA powders contained other calcium phosphate phases (amorphous and crystalline) apart from hydroxyapatite. The flow properties and stability of spheroidized HA were better than calcined HA and spray-dried HA. Standard metallographic preparation of the cross sections of the coatings revealed different microstructural features among the coatings. The HA coatings prepared from calcined HA were highly porous and lacking in intimate lamellar contact. The spheroidized HA powders produced the coating with the lowest porosity. Characterization of the powders and coatings was carried out using x-ray diffraction (XRD), scanning electron microscopy (SEM), and optical microscopy.**

**Keywords** hydroxyapatite, microstructure, phase composition, plasma spray, powder morphology

## 1. Introduction

HYDROXYAPATITE (HA) is emerging as an important biomaterial for numerous medical applications, such as orthopaedic and dental implants (Ref 1-6). It has favorable osteoconductive and bioactive properties that promote rapid bone formation and strong biological fixation to bony tissues (Ref 7, 8). Its chemical similarity to natural bone is aptly suited for musculo-skeletal bone substitution and reconstruction (Ref 9). There have been no adverse reports concerning cytotoxicity effects of HA (Ref 10). Although certain limitations in its intrinsic properties have restricted high stress or load bearing applications, recent development involving revolutionary concepts in prosthetic design and advanced surface technology are creating new ways and possibilities of incorporating HA to be used in conjunction with high stress metallic members to enhance osseointegration (Ref 11, 12).

HA coatings can be applied in several ways, but deposition via thermal spraying is the preferred choice (Ref 13-17). Although HA coating was conceived as a simple technique, wide variability in operating parameters often can induce unfavorable physiochemical transformations that can alter the biocompatibility and mechanical behavior of the HA coatings. Past studies have found undesirable phenomena, such as formation of amorphous calcium phosphate (ACP), tricalcium phosphate (TCP), and tetracalcium phosphate (TTCP) with concomitant reduction of the crystalline HA phase, deviation of the Ca/P stoichiometry, residual stresses, and occurrence of dehydroxylation (Ref 18-23). These detrimental consequences will reduce the potency of the HA coatings on the implants. The reduction of crystalline HA and deviation of the Ca/P stoichiometry would likely reduce the bioactive property and biocompatibility of the coatings while residual stresses could lead to premature mechanical failure of the coatings. A recent study showed the dependence of the crystalline HA phase and impurity phase amounts when different plasma forming gases were used (Ref 24). Another study suggested that loss of structural water during plasma spraying results in the formation of an OH-depleted hydroxyapatite. At high plasma power, $P_2O_5$, is lost, and the coatings contain increasing amounts of CaO and $Ca_4P_2O_9$ (Ref 25). Good cohesive and adhesive coating properties generally necessitate adequate melting of the powder to generate a consistent deposition of smooth and well-flattened lamellar splats. Present thermal spray processing techniques show that this is related to the formation of the more soluble amorphous phases. On this basis, a crystalline coating would be highly porous and mechanically weak because of poor cohesion between unmelted particles.

The short-term postoperative healing properties of HA are perhaps the most significant contribution to implant development (Ref 26, 27). The extent of this contribution is particularly sensitive to phase composition and crystallinity of the HA coating. Any anticipated long-term benefits are expected to depend on the adhesive and cohesive integrity of the coating, which are strongly microstructural dependent. Furthermore, long-term performance is determined by phase content, porosity, and residual stress of the coating.

The critical dependence of powder morphology and spray parameters to coating microstructure suggests the need for closer control and optimization of the thermal spraying process to attain the desired coating functionality (Ref 28, 29). This is particularly true for the HA coatings where great variability is observed when spray parameters are altered.

**P. Cheang,** School of Applied Science, Nanyang Technological University, Singapore 63 9798, Singapore; and **K.A. Khor,** School of Mechanical and Production Engineering, Nanyang Technological University, Singapore 63 9798, Singapore.

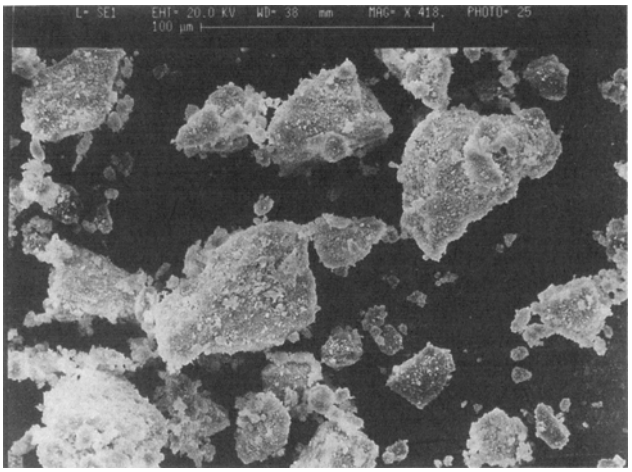

(a)

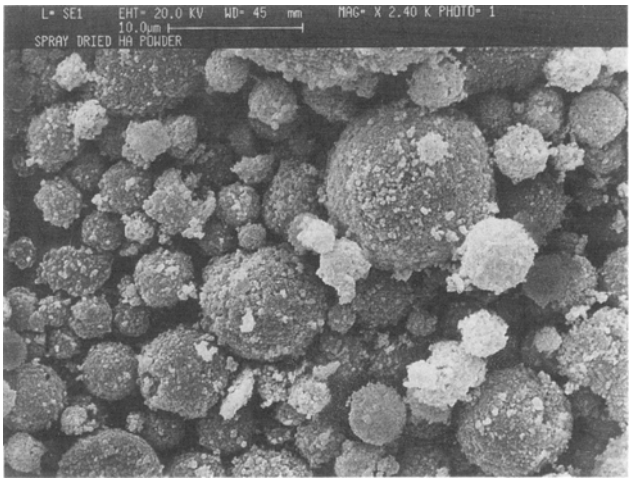


(b)

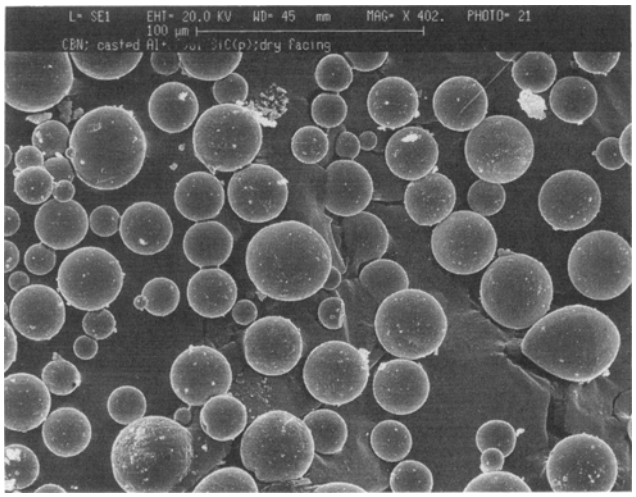

(c)

**Fig. 1** Particle morphology of HA powders: (a) calcined HA, (b) spray-dried HA, and (c) spheroidized HA

This study investigates the effect of powder configuration on the deposition behavior, coating microstructure, and phase composition of plasma sprayed HA coatings by using different HA powders as feedstocks.

## 2. Experimental Technique

Three different types of powder were used in this study. They were calcined HA (CHA), spheroidized HA (SHA), and spray-dried (SDHA). All were made from the same starting material produced by reacting orthophosphoric acid with calcium hydroxide. The resultant precipitate was dried at 180 °C, calcined at 800 °C for 4 h, and ground to various sizes in mortar and pestle. The CHA powder was produced to a particle size range of 53 to 75 μm. SHA was produced by flame spraying (Miller FP73 flame torch, Miller Thermal, Inc., Appleton, WI, USA) the calcined HA into distilled water. The spheroidized powders were sieved into two sizes: 20 to 45 μm and 45 to 53 μm. SDHA was prepared by ultrasonically dispersing the uncalcined HA and mixing it with a 2 wt% organic binder to form a slurry for spray drying (Lab-Plant SD-04, UK). The resultant SDHA powders

**Table 1 Plasma spraying condition**

| | |
|---|---|
| Main arc gas (argon) | 50 psi |
| Auxiliary gas (helium) | 15 to 50 psi |
| Arc current | 800 A |
| Arc voltage | 32 to 35 V |
| Spraying distance | 120 mm |
| Powder feed rate | 20 g/min |

**Table 2 Spray drying conditions**

| | |
|---|---|
| Spray dryer type | Two-fluid nozzle, concurrent flow |
| Nozzle diameter | 2 mm |
| Pump speed | $1.6 \times 10^{-4}$ m$^3$/h |
| Inlet temperature | 230 °C |
| Outlet temperature | 190 to 200 °C |
| Atomizing pressure | 4 bar |

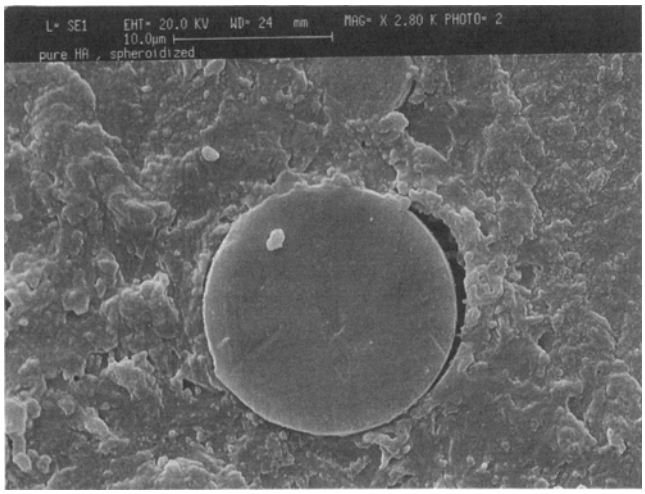


**Fig. 2** Polished cross section of a spheroidized HA powder

were calcined at 800 °C for 4 h to produce binder-free particulates of 5 to 20 μm.

The HA coatings were deposited using a 40 kW plasma torch (SG-100, Miller Thermal, Inc.) and powders delivered by a computerized closed-loop controlled rotor-feed hopper. All spraying conditions (Table 1) were similar, except in the amount of auxiliary gas (helium). Table 2 summarizes the spray drying conditions for production of the spray-dried HA powders.

Recovery rate of the powder from the spray drying operation is approximately 62%. Optical microscopy (Reichert Polyvar, Leica, Switzerland) and scanning electron microscopy (SEM) (Cambridge S360, Cambridge Instrument, UK) were used to evaluate the surface morphologies of coatings and powders. Polished cross sections of the coatings were prepared using standard metallographic procedures where the mounted samples were ground and polished with diamond-based pastes (9, 6, and 1 μm, respectively). The Philips MHD 1880 analytical XRD system (Philips Analytical, Almelo, The Netherlands) was used for phase characterization. Phase analysis was performed using nickel-filtered copper Kα radiation at 45 kV and 30 mA. The 2θ range from 20 to 80° was covered at a continuous scan speed of 0.1°/min. Density measurement was performed by the Ultrapycnometer P-1000 from Quantachrome (Quantachrome Corp., Boyton Beach, FL), that determined the volumetric displacement by the Archimedes principle using helium gas.

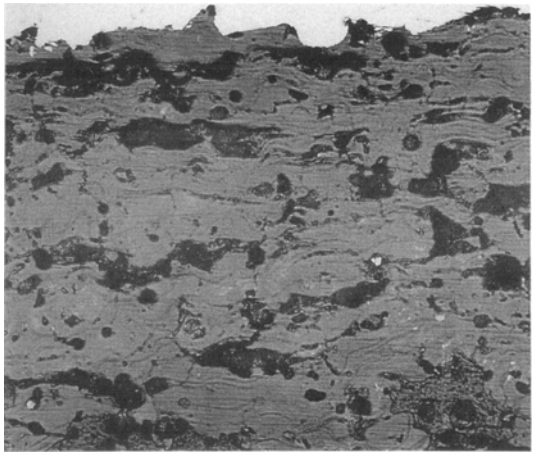

(a)

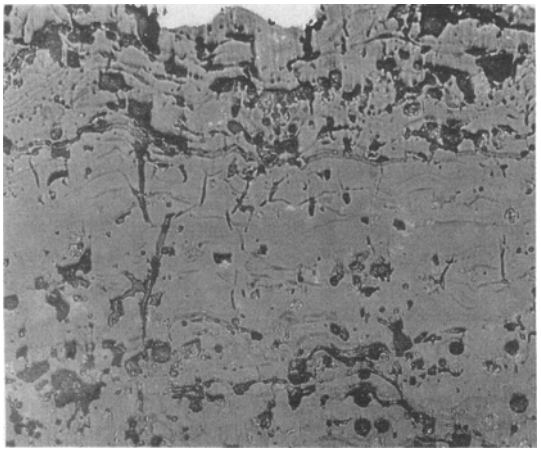

(b)

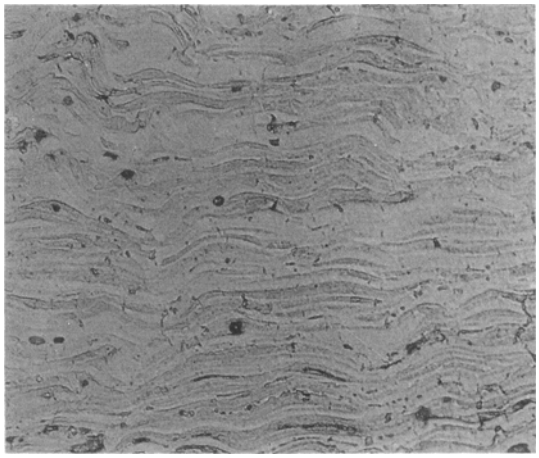

(c)

**Fig. 3** Coating microstructure of plasma sprayed HA· (a) calcined HA, (b) spray-dried HA, and (c) spheroidized HA

## 3. Results

The particle morphology of the different powders is shown in Fig. 1. The calcined HA (CHA) powders were irregular in shape and formed from an agglomeration of fine particles. They were porous and were in the size range from 53 to 75 μm. These agglomerated powders were structurally weak with a high tendency to break down in the plasma flame. The flowability of this angular powder was poor. The SHA and SDHA powders were mainly spherical in shape. In SHA powders, the main size distribution was between 20 and 53 μm. They were significantly smaller than the initial 53 to 75 μm feedstock used for spheroidization. The surface texture of these spherical particles was smooth and glassy. The internal particle structure was dense (Fig. 2). Particles above 45 μm were predominantly crystalline, whereas those below 45 μm were mainly amorphous. Their flow properties were extremely good. Tests conducted on the Hall flowmeter with SHA showed a flow rate of 0.45 g/s. This value is better than the values obtained in an earlier work with spray-dried hydroxyapatite powders where the flowability ranged from 0.11 to 0.27 g/s (Ref 30). SDHA powders were also spherical in shape but had rougher surface texture with a porous internal structure formed by the agglomeration of finer particulates. In addition, many porous cavities were created by the removal of the organic binder during debinding. SDHA powders ranged between 5 and 20 μm and had reasonably good flowability but poor strength. Table 3 lists the density of the powders used in this study. Results showed that the SHA powders have the highest density, and among the SHA powder size ranges, the 5 to 20 μm powders are the densest.

The cross-sectional microstructures of calcined, spray-dried, and spheroidized HA coatings are shown in Fig. 3(a), (b), and (c), respectively. There were considerable variations in the coating coherency between powders. The CHA coatings was highly porous and lacked intimate lamellar contact. The amount of porosity was lower in the spray-dried coating and lowest in the spheroidized HA coating. Image analysis of the coating micro-

structure showed that the highest coating defect density was in the CHA coating followed by the SDHA and SHA coating. SEM observation of the SDHA coatings showed evidence of incomplete melting among the particles that resulted in "pockets" of spherical particles (Fig. 4).

SEM images of the surface morphology of HA coatings are shown in Fig. 5. They revealed interesting features in splat formation and coating microstructure. With the SDHA powder, the irregular splat formation (Fig. 5b) produced an intricately porous microstructure (Fig. 3b). Coatings formed by the deposition of smooth and uniform SHA powder (Fig. 5c) produced a denser microstructure with the distinctive lamellar profile (Fig. 3c).

Figures 6(a), 6(b), and 7 show the respective microstructure of the SDHA and SHA coating sprayed at lower helium content. The lower helium gas content produced a less coherent microstructure of the SHA coating containing higher amounts of partially molten droplets in the form of unflattened splats of semicircular solids compared to Fig. 3(c).

Figure 8 shows the effect of particle size on coating microstructure. Both porosity and the amount of unmelted or partially melted particles were significantly higher using larger particles (45 to 53 μm) for the same spraying condition. The typical lamellar structure was less defined. Therefore, the larger size of the CHA powders, compared to SHA and SDHA, could in part explain the lower coating quality.

Figure 9 shows the XRD spectra of the plasma sprayed coatings. The calcined HA coating was less crystalline compared to the starting material. Additional phases, such as tricalcium phosphate (TCP), tetracalcium phosphate (TTCP), and calcium oxide (CaO), were also present. Compared with the spheroidized (45 to 53 μm) HA coating, the intensity of the main HA peak was

**Table 3 Density of HA powders in this study**

| Powder type | Density, g/cm$^3$ |
|---|---|
| Oven-dried HA, 180 °C, 12 h | 2.85 |
| Calcined HA, 800 °C, 4 h | 3.06 |
| Spray-dried HA, 2 to 20 μm | 3.11 |
| Spheroidized HA, 5 to 20 μm | 3.21 |
| Spheroidized HA, >20 μm | 3.15 |

Note: Theoretical density of crystalline HA is 3.219 g/cm$^3$

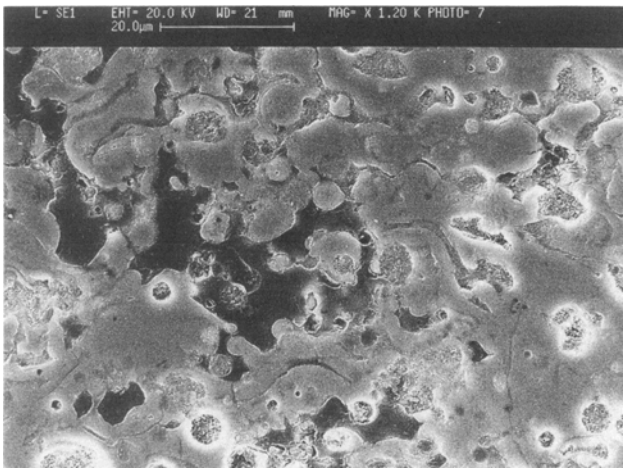


**Fig. 4** SEM micrograph of spray-dried HA coating cross section revealing "pockets" of unmelted particles

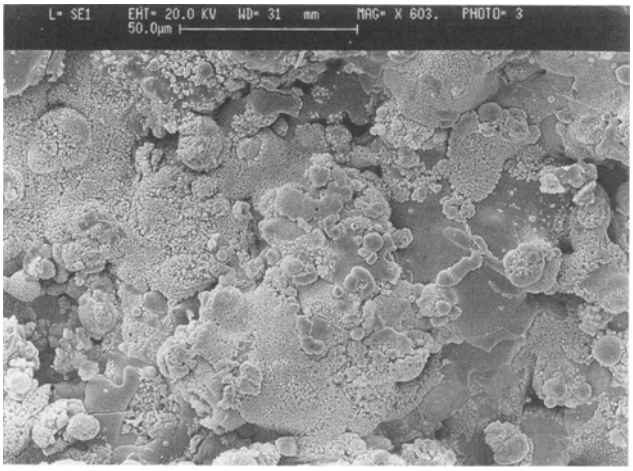


(a)

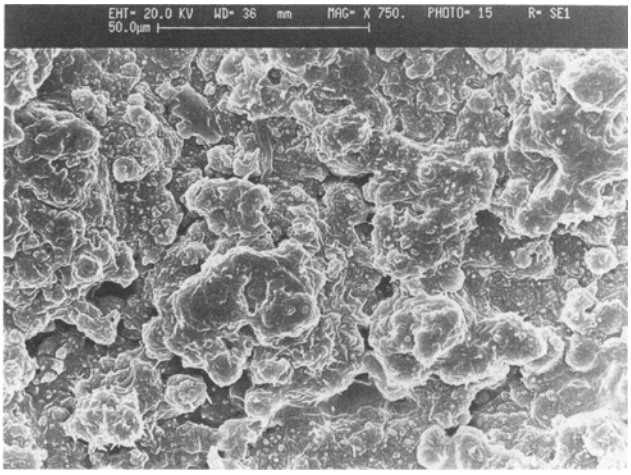


(b)

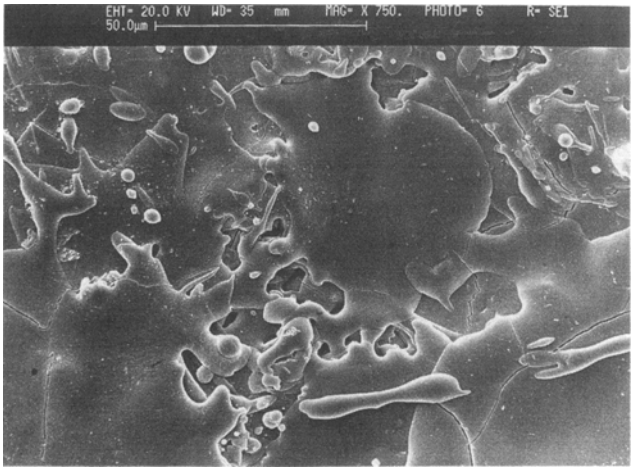


(c)

**Fig. 5** Surface morphology of plasma sprayed HA coatings: (a) calcined HA, (b) spray-dried HA, and (c) spheroidized HA

essentially the same, but the level of CaO was significantly lower. Changing to a smaller particle size (20 to 45 μm) significantly reduced the degree of crystallinity but did not seem to alter the amount of CaO with respect to crystalline HA. The CaO content was higher in the spray-dried HA coating, but the crystallinity was intermediate between SHA (45 to 53 μm) and SHA (20 to 45 μm).

## 4. Discussion

Examination of the plasma sprayed coatings revealed that the coating microstructure was sensitive to spray variables investigated in the present study, such as particle size range, particle morphology, initial powder density, and plasma gas composition. Microstructural features, such as porosity, splat profile, lamellar pattern, crystallinity, and phase composition, deviated according to powder morphology and plasma condition.

Coatings derived from agglomerated calcined powder (CHA) were incoherent with significant chemical variation (in particular the Ca:P ratio) shown by the formation of TCP, TTCP, and CaO. A previous study (Ref 19) on the plasma-particle interaction of agglomerated powders showed that the as-sprayed particle size distribution was in fact finer than the starting material. Agglomerated powders partially explode on entering the plasma because of the rapid expansion of entrapped gas in the pores and the thermal shock effect within the plasma environment; thus, tremendous stress is exerted on a mechanically weak structure. In addition, the phase formation was closely associated with the particle size. Particles above 75 μm were highly crystalline; those less than 30 μm were predominantly amorphous. Wide variations in the size of impacting particles and differences in

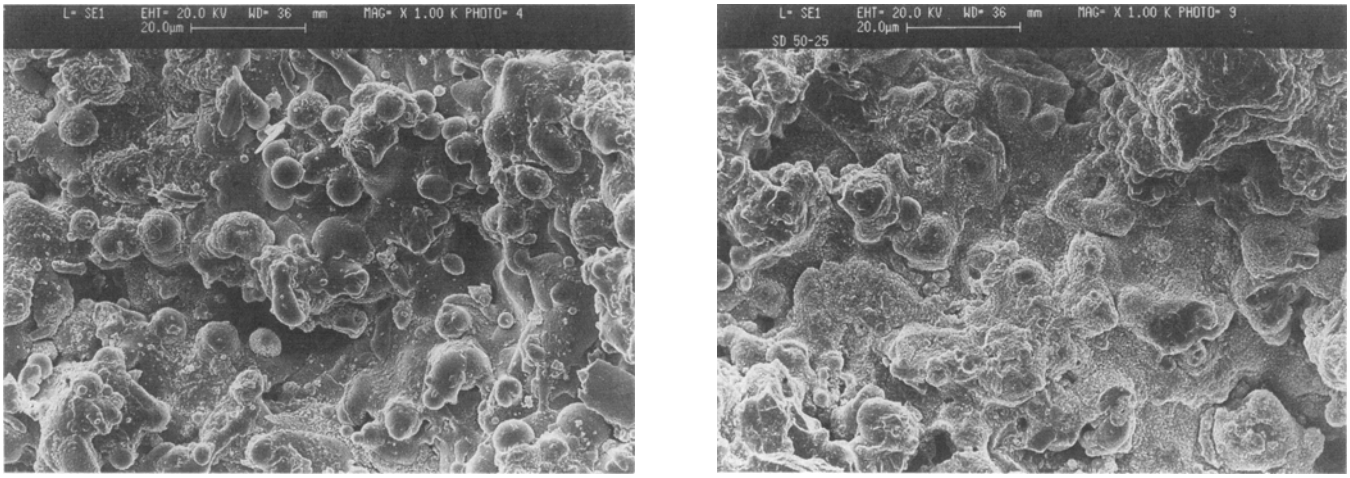


(a) (b)

**Fig. 6** Spray-dried HA coatings sprayed at lower helium auxiliary gas flow rates: (a) with 15 psi helium, and (b) with 25 psi helium

**Fig. 7** Spheroidized HA coating sprayed at lower helium auxiliary gas flow rate (338×)

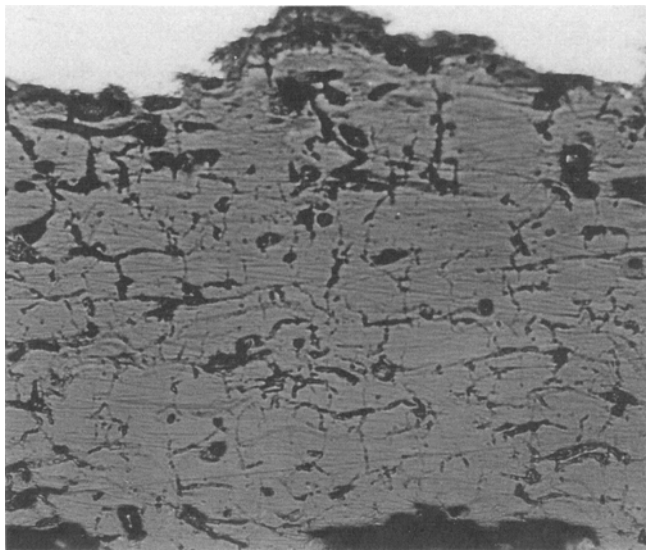

**Fig. 8** Spheroidized HA coating from larger particle sizes (45 to 53 μm) (338×)

physicochemical states contributed to a highly complex microstructure of micropores, deformed splats, and unmelted or partially melted particles. The poor powder characteristics of these irregular shaped agglomerates also reduced flowability and caused erratic and inconsistent deposition of material.

Using weakly agglomerated angular CHA powders did not produce good coating microstructure because of poor flowability and particle instability. Better flow characteristics were achieved using the better flowing, spherically shaped powders (SHA and SDHA). Spherical particles have good flowability, high deposition rate, and good melting characteristics. The spherical morphology offers consistent melting (Ref 31). Spray-dried HA powders have better flowability than angular CHA powders because of their circular geometry. Their higher strength compared to CHA also reduced the tendency for further breakdown. Spray-dried powders were structurally porous because of the binder agglomeration of finer particles. Burning off of the binder left behind hollow cavities. Surface and cross-section examination of SDHA coating revealed a porous microstructure (Fig. 3b, 4, 6a, and 6b). Although they are physically stronger than CHA, their thermal behavior is expected to be similar to agglomerated CHA. Irregularity in the size of impacting droplet and splat pattern suggests possible destabilization of the particles during spraying. XRD analysis showed that the coating was amorphous with a large concentration of CaO. This is certainly expected because of the 5 to 20 μm particle size, and it is also consistent with previous findings that smaller particle sizes generate higher amorphicity and CaO content (Ref 19).

The coating microstructure can be further improved using spheroidized particles. These powders are both dense and spherical with better flowability than SDHA because of the smoother particle surface. The spheroidizing process produces molten spherical droplets that fuse to a dense and strong body. The higher strength compared to CHA and SDHA increases the particle stability, which affects flowability during feeding and phase formation during plasma interaction. These coatings have high structural integrity because the spherical geometry provides uniform and consistent thermal treatment to produce fully molten conditions prior to impact. Selecting a particular particle size range can further minimize the formation of certain undesirable phases. Using a narrow and stable particle size range of 20 to 45 μm greatly reduced the formation of CaO, but an amorphous coating is inevitable. With larger particle size (45 to 53 μm), the crystallinity increases. All coatings generated from spheroidized HA were highly dense with very low porosity. The characteristic lamellar pattern in the coating verifies the formation of well-formed splats. The uniformity and stability of the particle size reduces the formation of porous cavities caused by uneven deposition. The sensitive relationship between coating microstructure and parameters suggests that an optimal spraying configuration exists for each powder morphology. For a 20 to 45 μm SHA powder, decreasing the heat content of the plasma by decreasing the helium content reduces the melting effect and thus promotes the formation of partially flattened sphere or teardrop shapes, which are less coherent. A similar outcome can be obtained using larger particles because of the higher heat content required for melting. Considerably thick coatings of up to 500 μm were successfully generated. Beyond this thickness, residual stresses are sufficient to initiate the formation of surface cracks, which propagate through the coating. The physical implication of such a dense microstructure is the improvement in mechanical property generated from these spheroidized powders.

The biological responses from these coating microstructures are not yet known. The resorption rate of amorphous coatings is expected to be high and to be further augmented by porosity. With such coatings, some form of postheat treatment may be necessary to reduce the transitional or high-temperature phases (TCP and TTCP) and, more importantly, restore the crystallinity or bioactive character so vital for postoperative healing (Ref 32). However, Brossa et al. (Ref 33) showed that heat treatment at 950 °C can introduce mechanical degradation of the HA coating although the crystallinity was increased. None of the pores generated were within the 100 to 200 μm size required for vascular bone ingrowth. Therefore its presence is of little value especially at the expense of mechanical strength. Efforts instead should be directed toward enhancing the structural integrity and bond strength by improving the coating microstructure.

The long-term benefits of a stable HA coating remains unclear. If it should become vital for long-lasting application, then the superior microstructural integrity derived using SHA powder may become important in the effort to achieve the ideal implant.

## 5. Conclusions

This study showed that powder characteristics of the HA powder feedstock markedly influence the coating microstructure and properties of hydroxyapatite. The coating microstructure can be improved by using dense spheroidized HA powder. Spheroidized HA powder provides better flowability and stability, which influences deposition and phase formation in the coating. The size of the powder feedstock has a significant

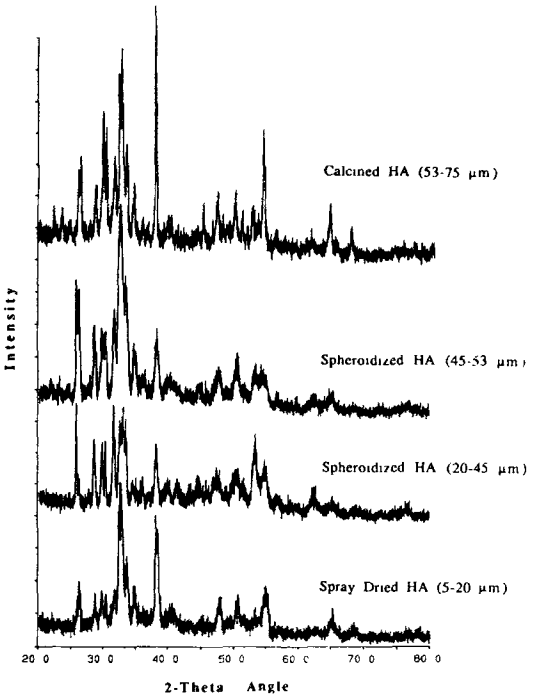


**Fig. 9** XRD spectra of HA coatings

effect on the phase composition, crystallinity, and porosity in the coating. The spherical shape and stability of this powder enhance the effect that particle size has in controlling the coating microstructure. The proportion of phase and crystallinity is often associated with a particular particle size range. Appropriate size selection often can be used to refine the resultant coating microstructure. However, any increase in crystallinity cannot be attained without some compromise in coating integrity with the plasma spraying conditions chosen for this work.

## Acknowledgments

Financial assistance from Nanyang Technological University in the form of applied research grant RP 56/92 is gratefully acknowledged. The authors wish to thank Chan Kok Leong, Ganasha Kumar, and Daniel Tay for their invaluable contribution and assistance.

## References

1. M. Kamegaya, Y. Shinohara, Y Shinada, H. Moriya, W. Koizumi,and K. Tsuchiya, The Use of Hydroxyapatite Block for Innominate Osteotomy, *J. Bone Joint Surg.*, Vol 76-B, 1994, p 123-126
2. R.G.T. Geesink and N.H.M. Hoefnagels, Six-Year Results of Hydroxyapatite-Coated Total Hip Replacement, *J. Bone Joint Surg.*, Vol 77-B (No. 4), 1995, p 534-547
3. P. Ducheyne, L.L. Hench, A. Kagan, M. Martens, A. Burssens, and J.C. Muller, The Effect of Hydroxyapatite Impregnation on Skeletal Bonding of Porous Coated Implants, *J. Biomed. Mater. Res.*, Vol 14, 1980, p 225-237
4. J.D. de Bruijn, C.A. van Blitterswijk, and J.E. Davis, Initial Bone Matrix Formation at the Hydroxyapatite Interface in vivo, *J. Biomed. Mater. Res.*, Vol 29, 1995, p 89-99
5. L.L. Hench, Bioceramics: From Concept to Clinic, *J. Am. Ceram. Soc.*, Vol 74 (No. 7), 1991, p 1487-1510
6. J.A. Antonio, W.N. Capello, O.D. Crothers, W.L. Jaffe, and M.T. Manley, Early Clinical Experience with Hydroxyapatite-Coated Femoral Implants, *J. Bone Joint Surg.*, Vol 74-A, 1992, p 995-1008
7. M. Muruyama, K. Terayama, M. Ito, T. Takei, and E. Kitagawa, Hydroxyapatite Clay for Gap Filling and Adequate Bone Ingrowth, *J. Biomed. Mater. Res.*, Vol 29, 1995, p 329-336
8 H.W. Denissen, W. Kalk, A.A.H. Veldhuis, and A. van der Hoff, Eleven Years of Study of Hydroxyapatite, *J. Prosthet. Dent.*, Vol 61 (No. 6), 1989, p 706-714
9. D.H. Kohn and P. Ducheyne, Materials for Bone and Joint Replacement, *Materials Science and Technology*, Vol 14, D.F. William, Ed., VHC Publishers, 1992, p 62-70
10. E. Lugscheider, M. Knepper, B. Heimberg, A. Dekker, and C.J. Kirkpatrick, Cytotoxicity Investigations of Plasma Sprayed Calcium Phosphate Coatings, *J. Mater. Sci.: Mater. Med.*, Vol 5, 1994, p 371-375
11. J.G.C. Wolke, K. van Dijk, H.G. Schaeken, K. de Groot, and J.A. Jansen, Study of the Surface Characteristics of Magnetron-Sputter Calcium Phosphate Coatings, *J. Biomed. Mater. Res.*, Vol 28, 1994, p 1477-1484
12. M.G.S. Murray, J. Wang, C.B. Ponton, and P.M. Marquis, An Improvement in Processing of Hydroxyapatite Ceramics, *J. Mater. Sci.*, Vol 30, 1995, p 3061-3074
13. C.P.A.T. Klein, P. Patka, J.G.C. Wolke, J.M.A. de Blieck-Hogervorst, and K. de Groot, Long Term in vivo Study of Plasma Sprayed Coatings on Titanium Alloys of Tetracalcium Phosphate, Hydroxyapatite and α-Tricalcium Phosphate, *Biomater.*, Vol 15, 1994, p 146-150
14. K. de Groot, C.P.A.T. Klein, J.G.C. Wolke, and J.M.A. de Blieck-Hogervorst, Plasma Sprayed Coatings of Calcium Phosphate, *CRC Handbook of Bioactive Ceramics: Calcium Phosphate and Hydroxyapatite Ceramics*, Vol II, T. Yamamuro, L.L. Hench, and J. Wilson, Ed., CRC Press, 1990, p 132-142
15. K. de Groot, R.G.T. Geesink, C.P.A.T. Klein, and P. Serekian, Plasma Sprayed Coatings of Hydroxyapatite, *J. Biomed. Mater. Res.*, Vol 21, 1987, p 1375
16. K.A. Gross and C.C. Berndt, Thermal Spraying od Hydroxyapatite for Bioceramic Applications, *Key Eng. Mater.*, Vol 124, 1991, p 53-55
17. J.D. Haman, L.C. Lucas, and D. Crawmer, Characterisation of High Velocity Oxy-Fuel Combustion Sprayed Hydroxyapatite, *Biomater.*, Vol 16, 1995, p 229-237
18. S.R. Radin and P. Ducheyne, Plasma Spraying Induced Changes of Calcium Phosphate Ceramic Characteristics and the Effect on in vitro Stability, *J. Mater. Sci.: Mater. Med.*, Vol 3, 1992, p 33-42
19. K.A. Khor and P.H.N. Cheang, Characterisation of Thermal Sprayed Hydroxyapatite Powders and Coatings, *J. Therm. Spray Technol.*, Vol 3 (No. 1), 1994, p 45-50
20. W. Tong, J. Chen, and X. Zhang, Amorphorization and Recrystallization During Plasma Spraying of Hydroxyapatite, *Biomater.*, Vol 16 (No. 11). 1995, p 829-832
21. B. Koch, J.G.C. Wolke, and K. de Groot, X-Ray Diffraction Studies on Plasma Sprayed Calcium Phosphate-Coated Implants, *J. Biomed. Mater. Res.*, Vol 24, 1990, p 655-667
22. S.R. Brown, I.G. Turner, and H. Reiter, Residual Stress Measurement in Thermal Sprayed Hydroxyapatite Coatings, *J. Mater. Sci.: Mater. Med.*, Vol 5, 1994, p 756-759
23. M. Weinlaender, J. Beumer, E.B. Kenney, P.K. Moy, and F. Adar, Raman Microprobe Investigation of the Calcium Phosphate Phases of Three Commercially Available Plasma-Flame-Sprayed Hydroxyapatite-Coated Dental Implants, *J. Mater. Sci.: Mater. Med.*, Vol 3, 1992, p 397-401
24. C.Y. Yang, B.C. Wang, E. Chang, and J.D. Wu, The Influences of Plasma Spraying Parameters on the Characteristics of Hydroxyapatite Coatings: A Quantitative Study, *J. Mater. Sci.: Mater. Med.*, Vol 6, 1995, p 249-257
25. R. McPherson, N. Gane, and T.J. Bastow, Structural Characterisation of Plasma Sprayed Hydroxyapatite Coatings, *J. Mater.Sci.: Mater. Med.*, Vol 6, 1995, p 327-334
26. R.G.T. Geesink, in *Hydroxyapatite Coated Hip Implants: Experimental and Clinical Studies*, P. Ducheyne, T. Kokubo, and C.A. van Blitterswik, Ed., Reed Healthcare Communications, 1992, p 121-138
27. S.D. Cook, K.A. Thomas, J.E. Dalton, T.K. Volkman, T.S. Whitecloud, and J.F. Kay, Hydroxyapatite Coating of Porous Implants Improves Bone Ingrowth and Interface Attachment Strength, *J. Biomed. Mater. Res.*, Vol 26, 1992, p 989-1001
28. M. Vardelle, A. Vardelle, and P. Fauchais, Spray Parameters and Particle Behavior Relationships During Plasma Spraying, *J. Therm. Spray Technol.*, Vol 2 (No. 1), 1993, p 79-91
29. E. Lugscheider, I. Rass, H.L. Heijnen, P. Chandler, T. Cosak, P. Fauchais, A. Denoirjean, and A. Vardelle, Comparison of the Coatings Properties of Different Types of Powder Morphologies, *Thermal Spray: International Advances in Coatings Technology*, C.C. Berndt, Ed., ASM International, 1992, p 967-973
30. E. Lugscheider, M. Knepper, and K.A. Gross, Production of Spherical Apatite Powders—The First Step for Optimised Thermal-Sprayed Apatite Coatings, *J. Therm. Spray Technol.*, Vol 1 (No. 3), 1992, p 215-221
31. M.R. Dorfman and J.D. Reardon, Spherical Ceramic Powders for Thermal Spraying, *Advances in Thermal Spraying (Proc. ITSC '86)* (Montreal Canada), The Welding Institute of Canada, 1986, p 241-249
32. P. Cheang and K.A. Khor, Thermal Spraying of Hydroxyapatite (HA) Coatings, *J. Mater. Proc. Technol.*, Vol 48, 1995, p 429-436
33. F. Brossa, A. Cigada, R. Chiesa, L. Paracchini, and C. Consonni, Post-Deposition Treatment Effects on Hydroxyapatite Vacuum Plasma Spray Coatings, *J. Mater. Sci.: Mater. Med.*, Vol 5, 1994, p 855-857